




# Remelting of Aluminum Scrap Into Billets Using Direct Chill Casting

Kardo Rajagukguk<sup>a, b, d</sup> , Suyitno Suyitno<sup>c, d, \*</sup>, Harwin Saptoadi<sup>a</sup>, Indraswari Kusumaningtyas<sup>a</sup>, Budi Arifvianto<sup>a, d</sup>, Muslim Mahardika<sup>a, d</sup>

<sup>a</sup> Department of Mechanical and Industrial Engineering, Faculty of Engineering, Universitas Gadjah Mada, Jl. Grafika 2, Yogyakarta 55281, Indonesia

<sup>b</sup> Department of Mechanical Engineering, Institut Teknologi Sumatera (ITERA), Jl. Terusan Ryacudu, South Lampung, Lampung 35365, Indonesia

<sup>c</sup> Department of Mechanical Engineering, Faculty of Engineering, Universitas Tidar, Jl. Kapten Suparman 39, North Magelang, 56116, Indonesia

<sup>d</sup> Center for Innovation of Medical Equipment and Devices (CIMEDs), Universitas Gadjah Mada, Jl. Teknik Utara Yogyakarta 55281, Indonesia

\* Corresponding author: E-mail address: [suyitno@untidar.ac.id](mailto:suyitno@untidar.ac.id)

Received 10.07.2023; accepted in revised form 27.11.2023; available online 04.03.2024

## Abstract

An as-cast aluminum billet with a diameter of 100 mm has been successfully prepared from aluminum scrap by using direct chill (DC) casting method. This study aims to investigate the microstructure and mechanical properties of such as-cast billets. Four locations along a cross-section of the as-cast billet radius were evaluated. The results show that the structures of the as-cast billet are a thin layer of coarse columnar grains at the solidified shell, feathery grains at the half radius of the billet, and coarse equiaxed grains at the billet center. The grain size tends to decrease from the center to the surface of the as-cast billet. The ultimate tensile strength (UTS) and the hardness values obtained from this research slightly increase from the center to the surface of the as-cast billet. The distribution of Mg, Fe, and Si elements over the cross-section of the as-cast billet is inhomogeneous. The segregation analysis shows that Si has negative segregation towards the surface, positive segregation at the middle, and negative segregation at the center of the as-cast billet. On the other hand, the Mg element is distributed uniformly in small quantities in the cross-section of the as-cast billet.

**Keywords:** Direct chill casting, Recycling aluminum scrap, Microstructure, Mechanical properties, Macrosegregation

## 1. Introduction

Nowadays, aluminum alloys are increasingly used as lightweight construction materials because they have excellent thermal and electrical conductivity, corrosion resistance, recyclability and high strength-to-weight ratio under atmospheric conditions [1–3]. The high demand for wrought aluminum products encourages the foundry industry to utilize aluminum

scrap as recycled material since it can reduce the cost of production [4]. According to data from the International Aluminum Institute (2019), a third of the aluminum used today is produced from recycled scrap, with this percentage expected to rise to 50% by 2050 [1,5]. Recycling aluminum end-of-life scrap is becoming popular to save natural resources, reduce production energy and reduce CO<sub>2</sub> emissions [6].

A third of the aluminum used today is made from recycled scrap and most of the aluminum scrap nowadays is from post-



consumer scrap [7]. The type of scrap that is frequently found in the surrounding environment comes from automotive, building construction, cookware and aluminum electronic components. An aluminum scrap from building and construction is one of the largest contributors to aluminum waste. This aluminum scrap is typically obtained from unused pieces of aluminum profiles, which are frequently used in building architecture such as for the construction of doors and windows. The aluminum profiles usually are made from an aluminum alloy 6XXX series. The AA6XXX series alloys are popular in the extrusion industry due to their excellent workability and are commonly known as high-speed extrusion alloys [8]. The AA6XXX series consists of three main elements such as Mg, Si, and Fe. The widely varying composition of scrap is one of the biggest challenges to recycling aluminum. The alloy composition of Mg, Si, and Fe in the AA6XXX series is strictly monitored in the foundry industry in accordance with ASTM standards.

Generally, the problem during the remelting of the scrap AA6XXX is the presence of impurity elements (gas elements, like hydrogen, alkaline earth metals, like magnesium and calcium) and inclusions (oxides, borides, nitrides, carbides, and chlorides) from aluminum melt. Undesired elements may also present in remelting of aluminum scrap. The presence of contamination impurities is a concern, particularly for large amounts of aluminum scrap derived from post-consumer scrap [1,8]. The accumulation of undesired elements, such as Fe and Si are very difficult to avoid due to the low solubility in solid aluminum [9]. The recycling and refining of scraps must reduce impurities, especially iron, to an acceptable level [10]. The negative effect of the high Fe content is the enhanced probability of forming large particles of AlFeSi [8] since it can reduce the workability of the alloy. The presence of an intermetallic of these phases affects the surface quality and mechanical properties of the products [10,11]. An element Si, combined with Mg, plays an important role in the formation of Mg<sub>2</sub>Si or  $\beta$  phase, which is the main hardening precipitate in the alloy [8]. As a result, lower grades and qualities of recycled aluminum scrap will be retrieved due to the presence of impurities [12]. On the other hand, the demand for wrought aluminum alloy products increases for low impurities and a good combination of mechanical properties.

Nowadays, direct chill (DC) casting is one of the most promising casting methods for producing wrought aluminum billets [13,14] due to its advantage that it can control the macrosegregation and high-speed casting production rate. The DC casting parameter used in the industry varies depending on the alloy composition and billet size. Some of the important casting parameters in the direct chill casting process have been recognized for example the casting speed [13], water flow rate [15], melt temperature, alloy composition [16], and billet size [13]. The start-up phase of the DC casting process is a critical condition since it can determine the production of casting defects [17]. Some of the casting defects that might be resulted from the DC casting are pores, hot tears [18], macro-segregation [19], cold cracking [20], cold shuts [17], micro and macro crack [21], oxide inclusions, and porosity [22]. Based on the above description, the research aims to evaluate the DC casting process for remelting aluminum scrap AA6XXX. The chemical composition, macro and microstructure, macrosegregation, and mechanical properties of

the aluminum billet alloy were investigated to evaluate the DC casting process.

## 2. Experimental Procedures

The aluminum scrap that was used in this experiment is obtained from extruded aluminum scrap (post-consumer scrap). This scrap comes from the remaining pieces of aluminum in the manufacture of windows for houses or buildings. A manual sorting procedure was carried out based on the application of the aluminum product. In addition, the aluminum scrap is also separated from the plastic wrapping layer and other metal components such as the bolt and hinge that are made from steel. Then, the aluminum scrap with a mass of up to 20 kg was placed inside a 30 mm x 50 mm ceramic crucible and was melted at 750 °C. In this research, we did not use degassing, fluxing or in-line filtering and grain refiner. The slag of the aluminum melt is removed manually or with a traditional hand-casting spoon. Fig. 1 shows the schematic experimental of the DC casting process. The molten metal was poured into billet molding at 700 °C using a casting spoon while the bottom block was stationary initially. Both the casting spoon and bottom block are made of steel. When the molten metal was introduced into the mold and filled the mold up to the hot top, the cooling water was pumped into the mold using a water pump, and it flowed through a pipe and valve system with a flow rate of 30 l/min. The temperature of the cooling water is 25 °C. The bottom block started to drag downward after about 80 seconds when the billet shell formed. The casting process was started at a constant casting speed of 50 mm/min, and the casting speed was controlled using a motor drive speed controller. The billet is pulled at the constant casting speed to the required length while the melt is continuously poured into the mold at a rate that keeps the melt level in the hot top constant [23].

Four K-type thermocouples as shown in Fig. 1. were fixed in a steel hollow. The steel wire was solidified and moved downward synchronously with the billet during the DC casting process. The process parameters such as melt, pouring, mushy zone temperature, and solidifying temperature are measured and recorded by a data acquisition system (DAQ) connected to a personal computer. Optical Emission Spectrometry (OES) was used to measure the composition of aluminum billet.

For macrostructure and microstructure observations, the specimens were selected from the steady-state conditions (in the middle of the as-cast billet). Billets were sawed at horizontal sections and the slices were subsequently cut into smaller samples, as indicated in Figs. 2a-e. For the macrostructural examination, specimens were mechanically polished and etched by (10 wt.%) NaOH aqueous solution. The microstructure of the specimen was etched by (5 wt.%) HBF<sub>4</sub> aqueous solution and observed under an inverted microscope (Carl Zeiss Axio Vert. A1). Hereafter, the micrographs were taken to analyze the average grain size using Jeffries' model in ASTM E112 standard [24]. To analyze the coarse and fine-cell structures of the solute, four samples were cut along the radius: one near to the surface of the billet ( $r=45$ ), one at the middle outside radius ( $r=30$ ), one at the middle inside ( $r=15$ ), and one in the center of the billet ( $r=0$ ), as shown in Fig. 2c. A Scanning Electron Microscopy (SEM) Zeiss

Ultra Plus equipped with an energy dispersive spectroscopy (EDS) detector was performed to analyze the microstructure of the samples. Moreover, to determine the crystallographic structure of as-cast billet, a Quantitative X-ray diffractometer test machine (XRD) with Cu K $\alpha$  radiation, scan rate: 2° min<sup>-1</sup>, scan step size: 0.02° and scan angle range: 30°–90° measurements were performed with Panalytical XRD machine on the different location along the cross-section of the samples.

The macrosegregation is observed using Optical emission spectroscopy (Thermo ARL 3560 OES). The macrosegregation of Mg, Si, and Fe elements at different positions along the radial direction of the billet as shown in Fig. 2c. Horizontal rectangular in cross-section samples were cut along the diameter of the billet, with a dimension of 40 x 40 x 100 mm. Then samples were milled in 200 $\mu$ m steps to obtain a detailed macrosegregation profile in the subsurface region. The bulk macrosegregation profile was measured every 8–10 mm along the diameter of the billet [16]. Totally three measurements were taken for each position. In this study, the average values of segregation are reported in the form of relative segregation i.e. the deviation of the current Mg and Si concentration from the average alloy composition of a long cross-section of the as-cast billet.

For further investigation, the mechanical properties test using ASTM B557-02a standard including Ultimate Tensile Strength (UTS), Yield Strength (YS), and elongation of the as-cast billet

were conducted using tensile test machine (Zwick-Roell ZHU 250 kN, Germany) at a crosshead speed of 1 mm/min at room temperature. At least two samples at each position i.e., center, middle and the near surface of the as-cast billet cross-section were tested and the average value of these tests was considered as the achieving properties of the alloys. Brinell hardness tester (Zwick-Roell ZHU250CL, Germany) was used to measure the hardness along the billet diameter. The hardness measurement was examined on four different locations along the radius as cast billet as shown in Fig. 2c.

### 3. Result and Discussions

#### 3.1. Analysis of as-cast billet structure

Fig. 2a. shows an as-cast aluminum billet with a length of 700 mm and diameter of 100 mm successfully cast using the direct chill casting method. Fig. 3 shows the cross-section of the as-cast billet is selected and sliced from the billet center. Table 1 shows the composition of the as-cast billet from the bottom up to the top section. The chemical compositions were determined at the bottom, middle and top of the as-cast billet.

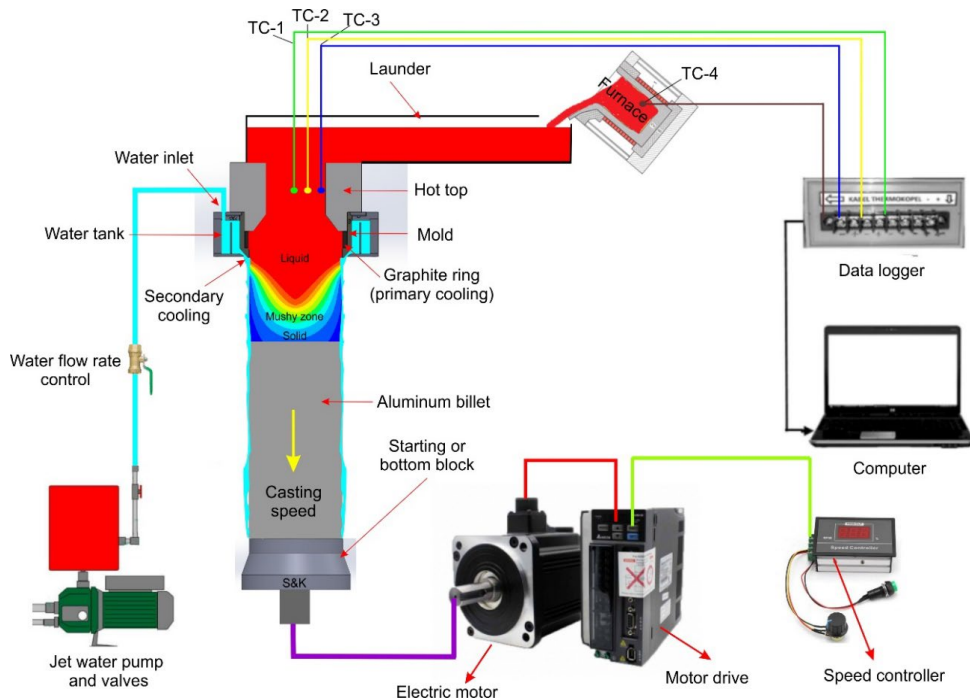


Fig. 1. Schematic experimental of direct chill casting process

Table 1. The composition (wt.%) of aluminum as-cast aluminum billet

As-cast Billet	Al	Si	Fe	Cu	Mn	Mg	Cr	Ni	Zn	Ti
Bottom	95.92	2.37	0.91	0.27	0.10	0.04	0.02	0.01	0.21	0.02
Middle	96.21	2.33	0.80	0.26	0.07	0.04	0.02	0.01	0.20	0.03
Top	95.98	2.26	0.94	0.27	0.10	0.03	0.02	0.01	0.22	0.02

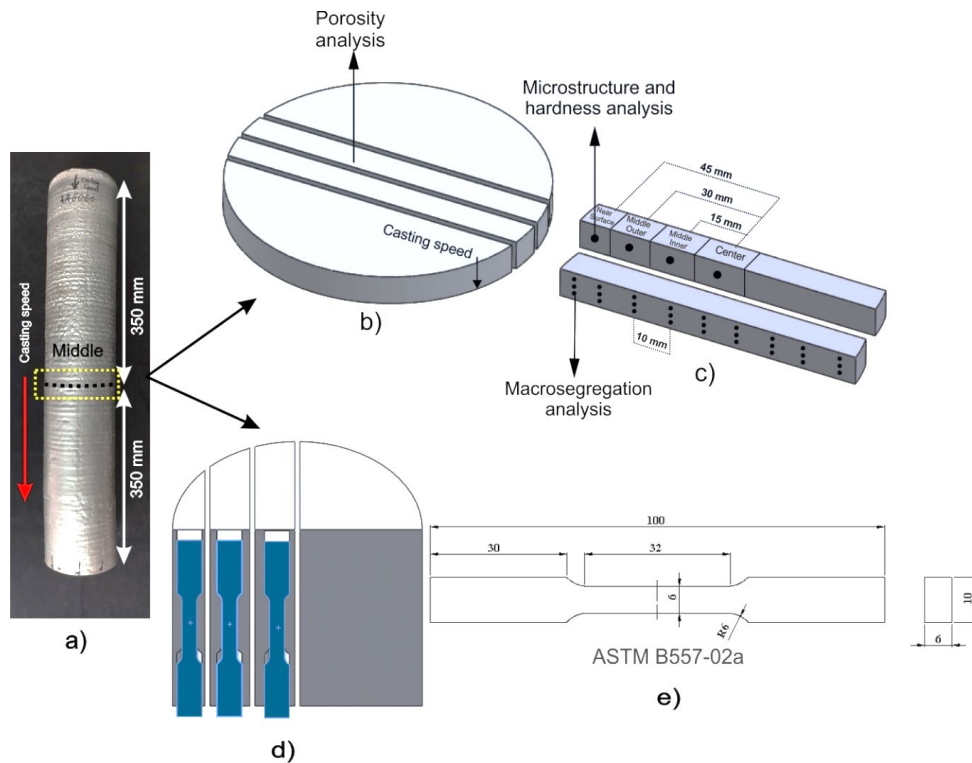


Fig. 2. Schematic diagram of material preparation and the position and dimension of the specimens. (a) as-cast billet (b) the porosity samples (c) the microstructure, hardness, and macrosegregation sample analysis (d) the tensile test sample, and (e) the standard dimension of tensile test

As can be seen in Fig. 3, the surface of the billet cross-section has no porosity. The porosity of as cast billet product was tested using the Archimedes method. The average porosity value is 0.279%. This measurement indicates that the as-cast billet product is close to the actual density of aluminum.

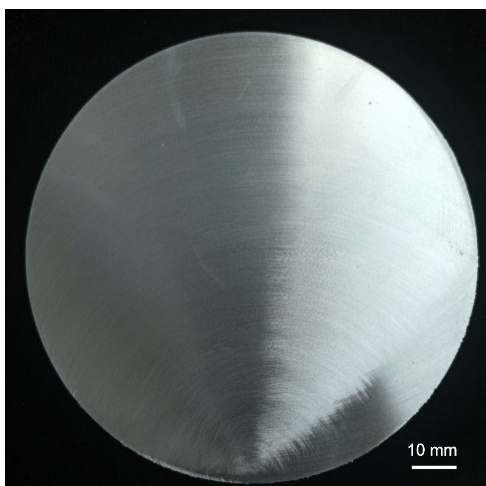


Fig. 3. Cross section of the as-cast billet

Fig. 4 shows the as-cast typical macrostructure along the cross-section of the billet product prepared by DC casting. The as-cast billet macrostructure shows a coarse and non-uniform grain

structure. Fig. 4 shows that there is a solidified shell near the billet surface. The thickness of the solidified shell is relatively thin, with an average thickness of 1-3 mm.

The structure around the solidified shell ( $r=45$ ) is a thin layer with coarse columnar grain and then the structure is transformed into feathery grains at the middle outside ( $r=30$  mm). At the billet center region ( $r=15-0$ ) the structure is coarse equiaxed grains. This observation is consistent with the previous works on DC casting in Ref. [22,25].

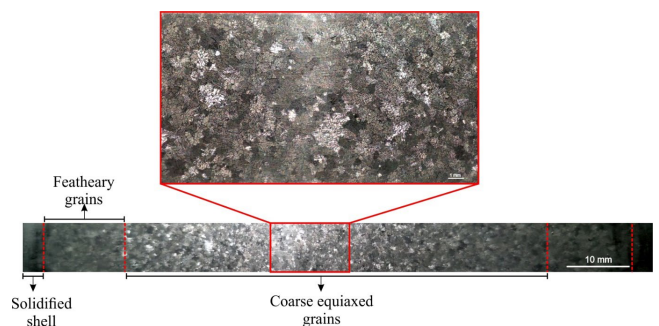


Fig. 4. As-cast typical macrostructure along the cross-section of billet diameter

Figs. 5a-d show the as-cast typical microstructures of the billet product at the position from the center ( $r=0$  mm), middle inside ( $r=15$  mm), middle outside ( $r=30$  mm), and near-surface ( $r=45$  mm). Fig. 5a illustrates clearly that the microstructure at the

center of the billet cast consists of coarse equiaxed grains. These grains contain thicker branches and greater dendritic arm spacing, with a rim of fine dendritic arm spacing around the grain's periphery [26]. As can be seen in Figs. 5b-c there are no significant differences in microstructure between the position at the middle inside and outside of the billet (range of  $r=15-30$  mm). The grain structure at the near-surface is finest than the others. The microstructure close to the billet surface is mainly composed of feathery grains that grow at an angle to the casting direction.

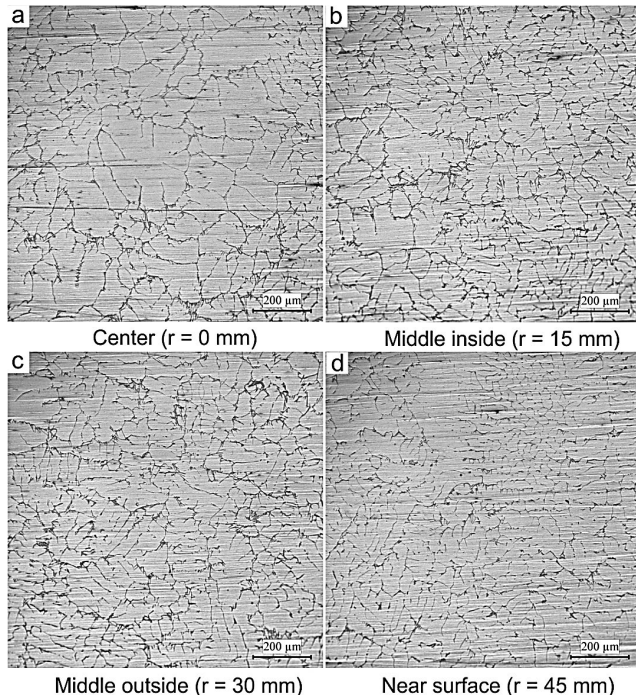


Fig. 5. As-cast microstructure of the aluminum billet. (a) Center ( $r=0$ ), (b) middle inside ( $r=15$  mm), (c) middle outside ( $r=30$  mm) and (d) near-surface ( $r=45$  mm)

The microstructural aspect of the material has a major influence on the performance of Al-alloys during the extrusion process as well as the qualities of the finished product [8]. In DC casting the grain structure depends on the alloy composition, grain refining, growth conditions and is also influenced by the cooling rate. The inhomogeneous distribution of cooling rates in the transition region is reflected in the inhomogeneous structure found in different sections of the billet [14]. The appearance of coarse grains in the center of a billet, as shown in Fig. 4 and Fig. 5 is caused by a slow cooling rate, leading the metal to take time longer to solidify and allowing dendrite that formed to grow and coarsen [19]. The slurry zone flow patterns produce scatter in solidification times and as a result, scatter in structural parameters related to cooling rate. Therefore, this explains the presence of coarse grains in the center of the billet. The feathery grain structure that forms at the middle outside is initiated by a high solidification rate and a slow flow [27]. On the other hand, at the periphery, the solid shell is formed by direct contact between the melt and the mold. It is formed into equiaxed grains due to its high cooling rate at the near surface of the as-cast billet [28].

Since the cooling rate is accelerated, the energy fluctuation and nucleation increase, so the liquid-solid phase transition takes place before the crystal grain grows up and resulting in fine grains [29].

The average grain size along the cross-section of the billet diameter from the center to the near surface is shown in Fig. 6. The average grain size from the center to the near surface of 88.9, 88, 75.4, and 74.3  $\mu\text{m}$  respectively. The grain size and morphology from the surface to the center of the billet changed significantly as shown in Fig. 5 and Fig. 6. The center of the billet has the biggest grain size, and the near-surface has the smallest grain size. However, the grain size does not change much between the middle inside and the near surface, this is also clearly seen in Figs. 5c-d. The grain size tends to increase from the surface to the center of the as-cast billet and this finding is also in line with Ref. [19,28,30,31]. Moreover, the grain size of the billet is progressively coarser from the surface to the center.

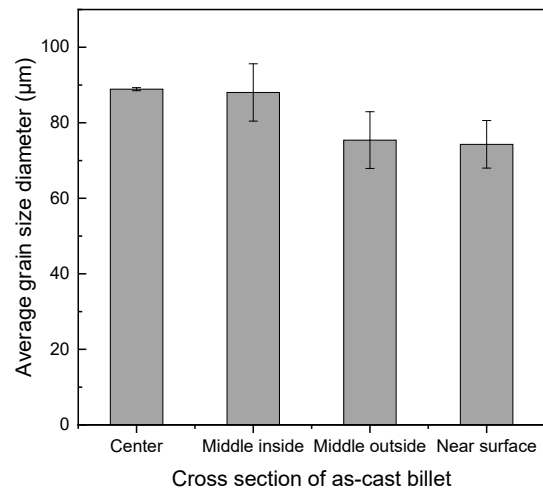


Fig. 6. Average grain size as a function of distance from the center of the billet cross-section

The grain size varies from the center to the surface of the as-cast billet due to the different cooling conditions encountered across the ingot's cross-section. The small grains as shown in Fig. 7d. caused due to the high heat loss rate between the primary mold and the billet surface. The grain size evolution with the cooling rate observed in this research is in good agreement with previous works on DC casting in Ref [2,19,26]. Increasing the cooling rate enhances both the inoculant nucleation potency in the melt and the density of active nucleation sites. From the DC cast parameter process variables, the water flow rate and casting speed have a minor effect on grain size variation [14].

For further microstructure analysis, Fig. 7 shows the SEM image of microstructures selected from various locations from the center of the ingot out towards the surface along the centerline of the cross-section of the billet. The alloy was composed of aluminum dendrite cells ( $\alpha$ -Al matrix) and large plate-like  $\beta$ - $\text{Al}_3\text{FeSi}$  intermetallic (gray) distributed along the dendrite boundaries. This finding indicates  $\text{Al}_3\text{FeSi}$  as the primary intermetallic phase in this as-cast billet alloy. This is also confirmed by the results of the XRD test as shown in Fig. 8.



Generally, it can be seen clearly that the structure coarsens toward the center of the billet.

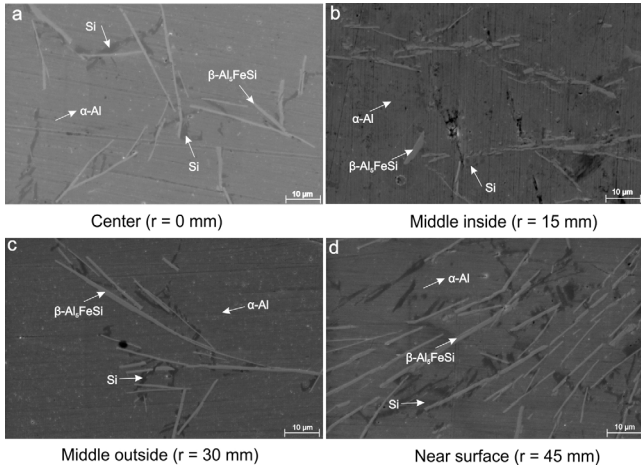


Fig. 7. Microstructure of direct chill as-cast billets corresponding to the location along the as-cast billet cross-section. (a) center, (b) middle inside, (c) middle outside and (d) near-surface

Fig. 8 shows XRD test results of the center, middle inside, middle outside, and near-surface location along the billet cross-section. A lower intensity with supplementary peaks at  $2\theta = 44.5^\circ$  at the center sample and  $2\theta = 82.2^\circ$  at the middle outside are identified to be characteristic of the  $Al_3FeSi$  fine precipitates with hexagonal structure. The XRD traces demonstrated that the intensities of the  $Al_3FeSi$  diffraction peaks varied with the tested region across the section of the as-cast billet.

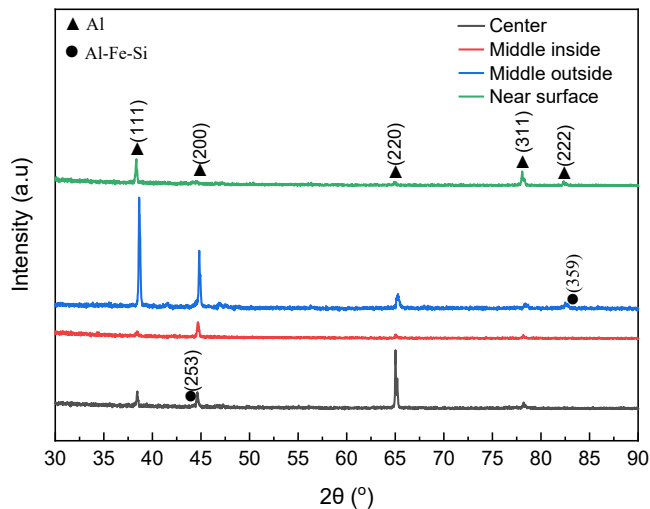
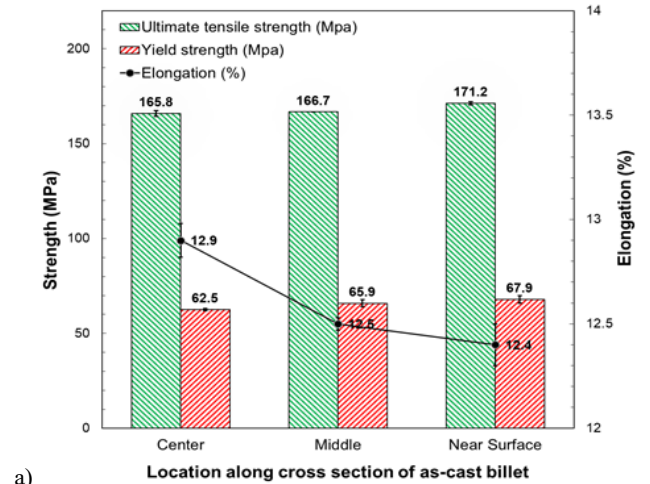


Fig. 8. X-ray diffractograms of the alloy in a different location along the cross-section of the billet.

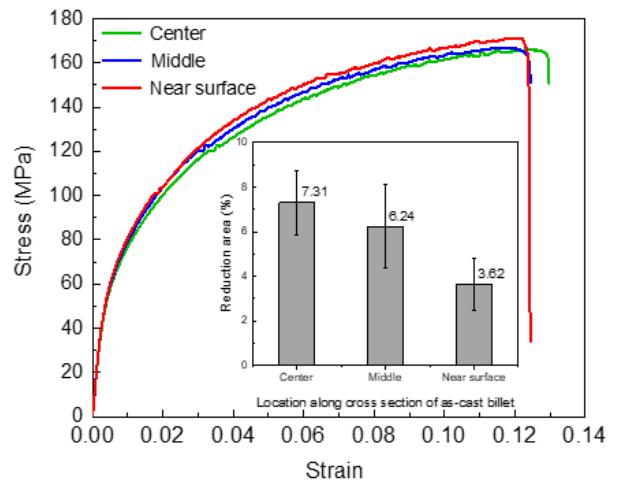
### 3.2. Mechanical properties of the as-cast billet

In this research, mechanical properties of the as-cast billet were characterized by using tensile and hardness tests. Fig. 9a

shows the tensile strength and elongation of the as-cast billet corresponding to the three locations across the section of the as-cast billet.



a)



b)



c)

Fig. 9. (a) Tensile test of direct chill cast billets on the various positions along the cross-section of the billet diameter, (b) stress-strain diagram, (c) tensile test samples after fracture

As can be seen, the near surface has the highest UTS of 171.2 MPa, while the center has the lowest tensile strength of 165.8 MPa. It is also seen that the UTS and YS increases slightly from the center to near surface. Meanwhile, the elongation decreases from the center to near surface. Fig. 9b shows the strain-stress

diagram of the as-cast billet. This graph also illustrates the reduction area of the tensile test samples using reduction area formula as defined in Eq. 1

$$\text{Percent reduction in area (\%)} = (A_0 - A_f) / A_0 \times 100 \quad (1)$$

where  $A_0$  represents the cross sectional area of the specimens and  $A_f$  represents the cross sectional area of the specimens when it finally ruptures (or breaks). This result confirms that the ductility decreases from the center to the near surface of the as-cast billet. Fig. 9c shows the tensile test sample corresponding to the three locations across the section of the billet.

The increasing trend in tensile test results can be attributed to the fact that the grain size of the billet decreases from the center to the near surface of as-cast billet [32] and it can be attributed to the cooling rate at the near surface of the billet is higher than the center which leads to the grain size being refined. The formation of brittle phases and faceted large platelets of  $\beta\text{-Al}_3\text{FeSi}$  Fe-rich intermetallics as shown in Fig. 7, in particular, reduces the ductility and ultimate tensile strength of cast products significantly [9]. On the other hand, macrosegregation of the DC casting billet has a detrimental influence on the mechanical properties of the DC casting billet [14].

Hardness tests were performed on as-cast billets at the bottom, middle, and top. Fig. 10 shows the average hardness on the bottom, middle, and top of as cast billet. As shown in Fig. 2c, the position hardness test was carried out along the cross-section of the billet radius. The average hardness value of the as-cast billet in this research is 45 HB, which is slightly higher than the hardness of the AA6063 as-cast billet prepared in works in Ref. [33,34].

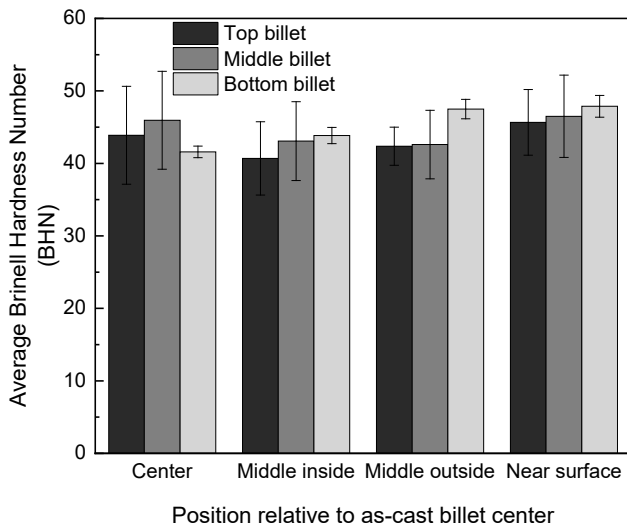


Fig. 10. The hardness along the cross-section of the as-cast billet

The near-surface has the highest average hardness value of 48.3 HB, whereas the center has the lowest. It can be seen that the hardness at the center has the lowest of all of the locations. Compared to the three locations of the billet, the top of the as-cast billet has the lowest average hardness.

As can be seen from Fig. 10 the hardness increases from the center to the near surface of the as-cast billet. This finding is also in line with the previous work in Ref. [33]. The element composition may be the main factor influencing material hardness in the as-cast microstructure. High hardness values are mainly obtained with small  $\alpha\text{-Al}$  grain sizes and high densities of submicroscopic  $\beta\text{-Mg}_2\text{Si}$  precipitates [35]. Given that coarse precipitation also affects the hardness values, although, to a lesser extent, the particle density for the coarse portion should be considered. The casting of aluminum alloys results in inhomogeneous alloying elements distribution in the microstructure, this is also caused by the varied hardness of a long billet cross-section. Therefore, homogenization treatment should be carried out on an as-cast billet to achieve homogeneous microstructure distribution. The technical literature reveals that the hardness value of alloys is a function that depends on grain size and the density and size of their precipitates. Table 2. shows the comparison mechanical properties data of as-cast aluminum billet formulated from aluminum scrap. In this research, no primary aluminum was added to the melt during the casting process.

Table 2.

The comparison on mechanical properties of as-cast billet formulated from aluminum scrap in our works with several previous works.

Mechanical properties	Recycled As-Cast Billet			
	AA6060 formulated from aluminum scrap [34]	AA6060 formulated from aluminum scrap and extruded into aluminum bar [8]	AA6063 formulated from 85% aluminum scrap with 15% aluminum ingots [33]	Our work use 100% aluminum scrap
Average UTS value	n/a	~220 MPa after aging 4 h	n/a	167.92 MPa
Average hardness value	39 HV	~35 HB	45.1 HV after homogenization	45 HB

### 3.3. Macrosegregation

Macrosegregation of Si and Mg is characterized using an index  $\Delta C$  (relative deviation), as defined in Eq. 1 in Ref. [19]:

$$\Delta C = (C_i - C_{ave}) / C_{ave} \quad (2)$$

where  $C_i$  represents the average of Si/Mg/Fe content at a test position and  $C_{ave}$  represents the average Si/Mg/Fe content of the ingot. Positive macrosegregation is indicated by values more than zero of this deviation, whereas negative macrosegregation is indicated by values less than zero. Fig. 11 shows the distribution of relative concentrations of Si, Mg, and Fe content along the

cross-section of the billet. As can be seen in Fig. 11, the distribution of Mg, Fe, and Si elements over the cross-section is inhomogeneous. The segregation ratio of Si has negative close to the billet surface and increases gradually to be positive segregation at the middle and negative segregation again at the center of the billet. The distribution of Mg content demonstrates negative segregation along the cross section from surface to center. Generally, Si and Fe tend to increase from the surface to the billet center. The content of the Mg element is distributed uniformly in small amounts along the cross-section of the as-cast billet.

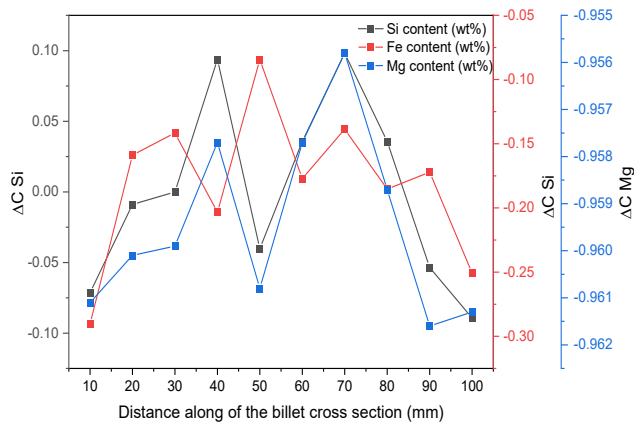


Fig. 11. Distribution of relative concentration Si, Mg, and Fe content along the cross-section of the billet

Macrosegregation is an irreparable and common defect [36] in billet prepared with DC castings. Macrosegregation is an inhomogeneous distribution of alloying elements at the solidified casting scale. This might result in non-uniform mechanical properties that affect the behavior of the metal during subsequent processing and decrease the quality of the final product. Macrosegregation is generally caused by the effect of solute redistribution during solidification, which is influenced by the movement of the solid and liquid phases in the mushy zone and the rejection of the solute by the solid phase [14]. Thermal convection [31], the movement of the solid phase in the liquid and slurry regions (which defines the distribution and volume fraction of ‘floating’ grains) [14], and the horizontal component of shrinkage-induced flow are the primary causes of centerline segregation in conventional DC casting. In general, the effects of floating grains and shrinkage-induced flow are major factors in the segregation, resulting in negative centerline segregation of ingots [31]. During the casting process, we were using a level melt entrance, which means that the melt flow enters a hot top from one side. This appears to cause some asymmetrical flows in the liquid pool, which may have implications for macrosegregation. This finding is also in line with Ref. [19]. Small particles of lower solute concentration separate from the first solidified shell and settle towards the center, resulting in macrosegregation. Due to gravity, the particles with a higher density as a result of the lower Mg concentration settle and move toward the base of the sump and finally, the negative macrosegregation in the center of the billet can further contribute to the decreased amount of eutectics. To improve the distribution

of elements in the billet alloy, it is strongly suggested that the billet should be homogenized first.

## 4. Conclusions

The remelting of aluminum scrap into billets using direct chill casting has been conducted. The conclusions are as follows:

1. The as-cast billet macrostructure has a coarse and non-uniform grain structure, with coarse columnar grain at the periphery that transforms into feathery grains at the middle outside and coarse equiaxed grains at the billet center.
2. The microstructures of the as-cast billet obtained by DC casting are mostly formed of aluminum dendrite cells (Al matrix) and large plate-like  $\beta$ -AlFeSi intermetallic.
3. The average grain size increases from the surface to the center of the billet.
4. The average hardness and ultimate tensile strength increase from the center to the surface of the billet.
5. Si has negative macrosegregation towards the surface and positive segregation at the middle and negative segregation again at the center of the billet. Mg content demonstrates negative segregation along the cross section from surface to center. Fe content tends to increase from the surface to the billet center.

Remelting aluminum scrap into billets using direct chill casting can be very promising. This potential can reduce production costs and environmental impact. However, based on the findings in this research, the presence of the  $\beta$ -Al<sub>3</sub>FeSi intermetallic phase and the macrosegregation element in as-cast billet are a problem which needs to be handled since it has a detrimental effect on the mechanical properties of the DC casting as-cast billet. Further efforts should be made to improve the quality of as-cast aluminum billet by utilizing aluminum scrap. Several works can be done such as controlling the raw material scrap, standardizing the alloy composition, refining the grain structure, and homogenizing the recycled as-cast billet after the direct chill casting process.

## Acknowledgments

This work was funded by The Ministry of Education and Culture, Republic of Indonesia with a research grant No. 1661/UN1/DITLIT/Dit-Lit/PT.01.03/2022, Universitas Gadjah Mada and Institut Teknologi Sumatera

## References

- [1] Raabe, D., Ponge, D., Uggowitzer, P., Roscher, M., Paolantonio, M., Liu, C., Antrekowitsch, H., Kozeschnik, E., Seidmann, D., Gault, B., De Geuser, F., Dechamps, A., Hutchinson, C., Liu, C., Li, Z., Prangnell, P., Robson, J., Shanthraj, P., Vakili, S. & Pogatscher, S. (2022). Making sustainable aluminum by recycling scrap: The science of “dirty” alloys. *Progress in Materials Science*. 128, 1-150, 100947. DOI:10.1016/j.pmatsci.2022.100947.



- [2] Jamaly, N., Haghdam, N. & Phillion, A.B. (2015). Microstructure, macrosegregation, and thermal analysis of direct chill cast AA5182 aluminum alloy. *Journal of Materials Engineering and Performance*. 24, 2067-2073. DOI: 10.1007/s11665-015-1480-7.
- [3] Vieth, P., Borgert, T., Homberg, W. & Grundmeier, G. (2022). Assessment of mechanical and optical properties of Al 6060 alloy particles by removal of contaminants. *Advanced Engineering Materials*. 25(3), 2201081. DOI: 10.1002/adem.202201081.
- [4] Wagstaff, R.S., Wagstaff, B.R. & Allamore, A. (2017). Tramp element accumulation and its effects on secondary phase particles. *The Minerals, Metals & Materials Society*. 1097-1103. DOI: 10.1007/978-3-319-51541-0.
- [5] Soo, V.K., Peeters, J., Paraskevas, D., Compston, P., Doolan, M. & Duflou, J.R. (2018). Sustainable aluminium recycling of end-of-life products: A joining techniques perspective. *Journal of Cleaner Production*. 178, 119-132. DOI: 10.1016/j.jclepro.2017.12.235.
- [6] Al-Helal, K., Patel, J.B., Scamans, G.M. & Fan, Z. (2020). Direct chill casting and extrusion of AA6111 aluminum alloy formulated from taint tabor scrap. *Materials*. 13(24), 5740, 1-11. DOI: 10.3390/ma13245740.
- [7] Graedel, T.E., Allwood, J., Birat, J.P., Buchert, M., Hagelüken, C., Reck, B.K., Sibley, S.F. & Sonnemann, G. (2011). What do we know about metal recycling rates? *Journal of Industrial Ecology*. 15(3), 355-366. DOI: 10.1111/j.1530-9290.2011.00342.x.
- [8] Silva, M.S., Barbosa, C., Acselrad, O. & Pereira, L.C. (2004). Effect of chemical composition variation on microstructure and mechanical properties of AA 6060 aluminum alloy. *Journal of Materials Engineering and Performance*. 13, 129-134. DOI: 10.1361/10599490418307.
- [9] Al-Helal, K., Lazaro-Nebreda, Patel, J. & Scamans, G. (2021). High-shear de-gassing and de-ironing of an aluminum. *Recycling*. 6 (66), 2-10. <https://doi.org/10.1111/j.1530-9290.2011.00342.x>.
- [10] Zhang, L., Gao, J., Damoah, L.N.W. & Robertson, D.G. (2012). Removal of iron from aluminum: A review. *Mineral Processing and Extractive Metallurgy Review*. 33(2), 99-157. DOI: 10.1080/08827508.2010.542211.
- [11] Zhang, L., Lv, X., Torgerson, A.T. & Long, M. (2011). Removal of impurity elements from molten aluminum: A review. *Mineral Processing and Extractive Metallurgy Review*. 32(3), 150-228. DOI: 10.1080/08827508.2010.483396.
- [12] Paraskevas, D., Kellens, K., Dewulf, W. & Duflou, J.R. (2015). Environmental modelling of aluminium recycling: A Life Cycle Assessment tool for sustainable metal management. *Journal of Cleaner Production*. 105, 357-370. DOI: 10.1016/j.jclepro.2014.09.102.
- [13] Eskin, D.G., Savran, V.I. & Katgerman, L. (2005). Effects of melt temperature and casting speed on the structure and defect formation during direct-chill casting of an Al-Cu alloy. *Metallurgical and Materials Transactions A*. 36, 1965-1976. DOI: 10.1007/s11661-005-0059-6.
- [14] Nadella, R., Eskin, D.G., Du, Q. & Katgerman, L. (2008). Macrosegregation in direct-chill casting of aluminium alloys. *Progress in Materials Science*. 53(3), 421-480. DOI: 10.1016/j.pmatsci.2007.10.001.
- [15] Eskin, D.G. (2014). Mechanisms and Control of Macrosegregation in DC Casting. *Light Metals 2014*. 855-860. DOI: 10.1002/9781118888438.ch143.
- [16] Mortensen, D., M'Hamdi, M., Ellingsen, K., Tveito, K., Pedersen, L. & Grasmø, G. (2014). Macrosegregation modelling of DC-casting including grain motion and surface exudation. *Light Metals 2014*. 867-872. DOI: 10.1002/9781118888438.ch145.
- [17] Jolly, M., & Katgerman, L. (2022). Modelling of defects in aluminium cast products. *Progress in materials science*. 123, 1-39. DOI: 10.1016/j.pmatsci.2021.100824
- [18] Suyitno, Kool, W.H. & Katgerman, L. (2005). Hot tearing criteria evaluation for direct-chill casting of an Al-4.5 pct Cu alloy. *Metallurgical and Materials Transactions A: Physical Metallurgy and Materials Science*. 36(6), 1537-1546. DOI: 10.1007/s11661-005-0245-6.
- [19] Eskin, D.G., Zuidema, J., Savran, V.I. & Katgerman, L. (2004). Structure formation and macrosegregation under different process conditions during DC casting. *Materials Science and Engineering A*. 384(1-2), 232-244. DOI: 10.1016/j.msea.2004.05.066.
- [20] Lalpoor, M., Eskin, D. G., Ruvalcaba, D., Fjær, H.G., Ten Cate, A., Ontijt, N. & Katgerman, L. (2011). Cold cracking in DC-cast high strength aluminum alloy ingots: An intrinsic problem intensified by casting process parameters. *Materials Science and Engineering A*. 528(6), 2831-2842. DOI: 10.1016/j.msea.2010.12.040.
- [21] Grandfield, J.F., Eskin, D.G, Bainbridge, I.F. (2013). *Direct-chill casting of light alloys*. United States of America: John Wiley & Sons, Inc., Hoboken, New Jersey. DOI: 10.1002/9781118690734.
- [22] Wang, R., Zuo, Y., Zhu, Q., Liu, X. & Wang, J. (2022). Effect of temperature field on the porosity and mechanical properties of 2024 aluminum alloy prepared by direct chill casting with melt shearing. *Journal of Materials Processing Technology*. 307, 117687. DOI: 10.1016/j.jmatprotec.2022.117687.
- [23] Barekar, N.S., Skalicky, I., Barbatti, C., Fan, Z. & Jarrett, M. (2021). Enhancement of chip breakability of aluminium alloys by controlling the solidification during direct chill casting. *Journal of Alloys and Compounds*. 862, 158008. DOI: 10.1016/j.jallcom.2020.158008.
- [24] ASTM E112. (2010). Standard test methods for determining average grain size E112-10. *ASTM E112-10*. 96(2004), 1-27. DOI: 10.1520/E0112-10.
- [25] Jones, S., Rao, A.K.P., Patel, J.B., Scamans, G.M. Fan, Z. (2012). Microstructural evolution in intensively melt sheared direct chill cast Al-alloys. *In the 13th International Conference on Aluminum Alloys (ICAA13) 2013*, (pp. 91-96). DOI: 10.1007/978-3-319-48761-8\_15.
- [26] Suyitno, A., Eskin, D.G., Savran, V.I. & Katgerman, L. (2004). Effects of alloy composition and casting speed on structure formation and hot tearing during direct-chill casting of Al-Cu alloys. *Metallurgical and Materials Transactions A*. 35 A(11), 3551-3561. DOI: 10.1007/s11661-004-0192-7.
- [27] Turchin, A.N., Zuijderwijk, M., Pool, J., Eskin, D.G. & Katgerman, L. (2007). Feathery grain growth during

- solidification under forced flow conditions. *Acta Materialia*. 55(11), 3795-3801. DOI: 10.1016/j.actamat.2007.02.030.
- [28] Liu, X., Zhu, Q., Jia, T., Zhao, Z., Cui, J. & Zuo, Y. (2020). As-cast structure and temperature field of direct-chill cast 2024 alloy ingot at different casting speeds. *Journal of Materials Engineering and Performance*. 29(10), 6840-6848. DOI: 10.1007/s11665-020-05140-x.
- [29] Tian L., Guo, Y., Li, J., Xia, F., Liang, M. & Bai, Y.(2018) Effects of solidification cooling rate on the microstructure and mechanical properties of a cast Al-Si-Cu-Mg-Ni piston alloy. *Materials*. 11(7), 3-11. DOI: 10.3390/ma11071230.
- [30] Suyitno. (2016). Effect of composition on the microporosity, microstructure, and macrostructure in the start-up direct-chill casting billet of Al-Cu alloys. *ARPN Journal of Engineering and Applied Sciences*. 11(2), 962-967. <https://doi.org/10.1007/s11661-004-0192-7>.
- [31] Zhu, C., Zhao, Z. hao, Zhu, Q. feng, Wang, G. song, Zuo, Y. bo, & Qin, G. wu. (2022). Structures and macrosegregation of a 2024 aluminum alloy fabricated by direct chill casting with double cooling field. *China Foundry*. 19(1), 1-8. DOI: 10.1007/s41230-022-1030-5.
- [32] Zheng, X., Dong, J. & Wang, S. (2018). Microstructure and mechanical properties of Mg-Nd-Zn-Zr billet prepared by direct chill casting. *Journal of Magnesium and Alloys*. 6(1), 95-99. DOI: 10.1016/j.jma.2018.01.003.
- [33] Arif, A.F.M., Akhtar, S.S. & Sheikh, A.K. (2009). Effect of Al-6063 billet quality on the service life of hot extrusion die: metallurgical and statistical investigation. *Journal of Failure Analysis and Prevention*. 9, 253-261. DOI: 10.1007/s11668-009-9231-4.
- [34] Triantafyllidis, G.K., Kiligaridis, I., Zagkliveris, D.I., Orfanou, I., Spyridopoulou, S., Mitoudi-Vagourdi, E. & Semertzidou, S. (2015). Characterization of the A6060 Al alloy mainly by using the micro-hardness vickers test in order to optimize the industrial solutionizing conditions of the as-cast billets. *Material. Science and Applications*. 06(01), 86-94. DOI: 10.4236/msa.2015.61011.
- [35] Asensio-Lozano J., Suárez-Peña, B. & Voort, G.F.V. (2014). Effect of processing steps on the mechanical properties and surface appearance of 6063 aluminium extruded products. *Materials*. 7(6), 4224-4242. DOI: 10.3390/ma7064224.
- [36] Založnik, M. & Šarler, B. (2005). Modeling of macrosegregation in direct-chill casting of aluminum alloys: Estimating the influence of casting parameters. *Materials Science and Engineering A*. 413-414, 85-91. DOI: 10.1016/j.msea.2005.09.056.